UNIVERSITY OF DELAWARE
INSTITUTE OF ENERGY CONVERSION
University of Delaware
Newark, DE 19716-3820
Ph: 302/831-6200
Fax: 302/831-6226
www.udel.edu/iec
UNITED STATES DEPARTMENT OF ENERGY
UNIVERSITY CENTER OF EXCELLENCE
FOR PHOTOVOLTAIC RESEARCH AND EDUCATION

June 6, 2005

Ken Zweibel
National Renewable Energy Laboratory
1617 Cole Boulevard
Golden, CO 80401

Re: NREL Subcontract #ADJ-1-30630-12

Dear Ken,

This report covers research conducted at the Institute of Energy Conversion (IEC) for the period of April 9, 2005 to May 9, 2005, under the subject subcontract. The report highlights progress and results obtained under Task 2 ($CuInSe_2$-based Solar Cells).

Task 2: $CuInSe_2$-based Solar Cells

In Line Evaporation System

Severe control problems have been encountered with the Cu source incorporating the new insulation scheme that was necessary for operation at the higher temperatures required for higher deposition rates. The unstable behavior was the same one observed during the previous years and was thought to have been resolved. The issue was traced to a design fault in the National Instrument's Field Point Thermocouple Module (FP-TC-120). In short, the module generates unstable temperature readings if the thermocouple voltage is more than 20mV and there is more than one thermocouple attached to the module. At the present time, the Cu control thermocouple is attached to an independent FP-TC-120 module in which seven other input ports are shorted. In this way, control instabilities were removed and the system became fully operational.

A number of depositions were performed on Mo-on-UpilexS substrates to recalibrate the system in terms of the $Cu(InGa)Se_2$ composition and device performance level. Mo coatings had two

different thickness, 2000Å and 1000Å. Table I gives the results obtained at the end of this recalibration process.

Table I. System calibration runs giving Cu(InGa)Se_2 composition and the best device characteristics.

Run	Mo Thck (Å)		At %	Ratio (M/III)	Best Device V_{oc} (V)	J_{sc} (mA/cm^2)	FF (%)	Eff (%)
70321	2000	Cu	24.2	0.90	0.554	31.3	57.1	9.9
		Ga	9.3	0.35				
		In	17.5					
		Se	49.1					
70322	2000	Cu	24.2	0.92	0.539	33.5	54.9	9.9
		Ga	10.7	0.41				
		In	15.6					
		Se	49.5					
70324	1000	Cu	25.5	0.99	0.546	31.6	47.2	8.2
		Ga	10.5	0.41				
		In	15.3					
		Se	48.7					

Lower device performance on 1000Å Mo may be due to the difficulty in making a back contact for probing without damaging the Mo layer. This point is presently under investigation. Nevertheless, the data shows that the system with the new source insulation can give reproducible compositions and acceptable device performance.

Another requirement on the sources for high temperature operation is that the vapors should not leak out through the joint between the lid and the body of the source. Presently, a small amount of leakage is observed but it does not result in any operational problem. However, at high rates of effusion, such a leak will reach unacceptable levels. As a result, a sealed source has been designed, which will be fabricated and tested during the next reporting period.

Wide Bandgap Materials: Cu(InAl)Se_2

Results were presented for the evaporation of Cu(InAl)Se_2 using a 3-stage process in the February 2005 report under this contract. However, this process is complicated in the baseline IEC evaporators by the relatively slow thermal response times of the insulated Knudsen-type sources. Thus, a simplified version of this process has been developed. In Figure 1, schematic temperature profile of the metal sources during this process is shown. The In and Al source temperatures are kept constant and determine the relative Al content. Once the shutter is opened, the Cu source temperature is ramped from 1100°C to a designated temperature (e.g. 1350°C in the case show) with a ramp rate of 10°C/min. Then T(Cu) is held constant. The final Cu

temperature is determined so that the impingement rate of Cu is higher than the sum of In and Al ([Cu]/[In+Al] >1) and the film composition changes from Cu poor to Cu rich. Figure 2 shows a typical substrate temperature profile during the deposition. Similar to the 3-stage process, the temperature changes under constant substrate heater power. Due to the formation and then consumption of Cu-Se phases, these changes can be measured and used for composition control. After the film becomes Cu-rich, the Cu source is turned off; and when the film becomes sufficiently Cu-poor again, the In and Al sources are turned off.

$Cu(InAl)Se_2$ films deposited with this process have similar morphology to those deposited with a 3-stage process. Device results will be presented in the next report. This process can be easily modified to start the deposition with different relative Cu-contents, as long as [Cu]/[In+Al] <1 at the start. This method will be used to study the effect of initial Cu concentration on adhesion since a correlation has been previously observed.

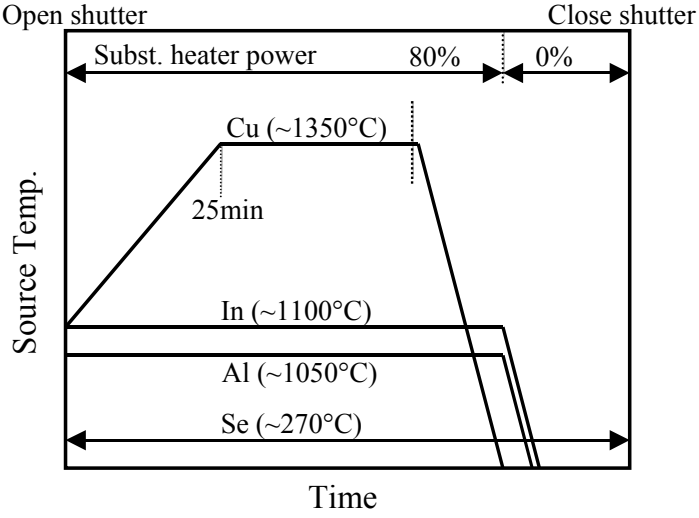

Figure 1. Source temperatures and substrate heater power during the deposition.

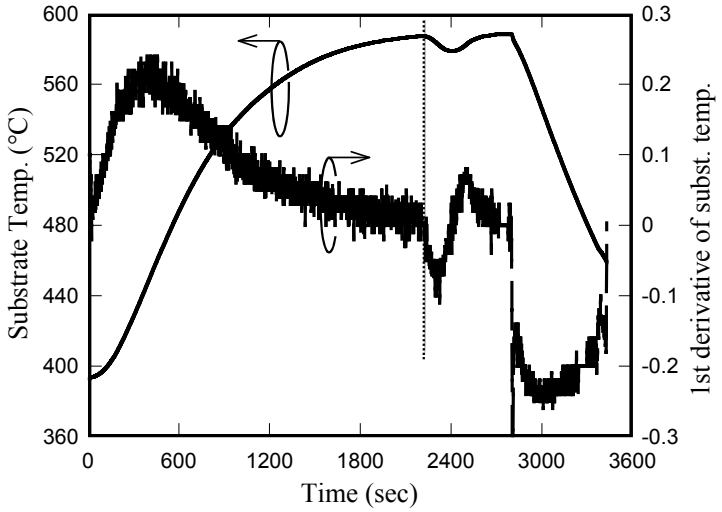

Figure 2. Substrate temperature profile during a Cu(InAl)Se_2 deposition using the profile in Figure 1.

Cu(InGa)$(SeS)_2$ Formation by H_2Se/H_2S Reaction

Characterization of the formation of Cu(InGa)$(SeS)_2$ by reaction of Cu-Ga-In precursor layers in H_2Se/H_2S continues, with the objective of developing a process to control through-film compositional uniformity of Cu(InGa)$(SSe)_2$ and increase device voltage. In this report characterization of the Cu-Ga-In precursor and selenized Cu(InGa)Se_2 films are presented.

Precursor characterization

Precursors were deposited by sequentially sputtering a Cu-Ga alloy film from a $Cu_{0.8}Ga_{0.2}$ target followed by an elemental In layer onto a Mo-coated soda lime glass substrate. The thicknesses of the films were 349 nm for the Cu-Ga film and 489 nm for the In film to give an overall composition of Cu/(In+Ga) = 0.9 and Ga/(In+Ga) = 0.225.

To approximate the Cu-Ga-In phase equilibrium at the reaction temperature, samples were heat treated in the absence of the hydride for 10 min in otherwise standard reactor conditions as defined below. Figure 3 shows the CuKα_1 x-ray diffraction (XRD) spectrum of one of these samples. The peak indices are shown in Table II. The detected phases include In and a Cu_9In_4-Cu_9Ga_4 alloy with composition $Cu_9(Ga_{0.36}In_{0.64})_4$ estimated by Vegard analysis.

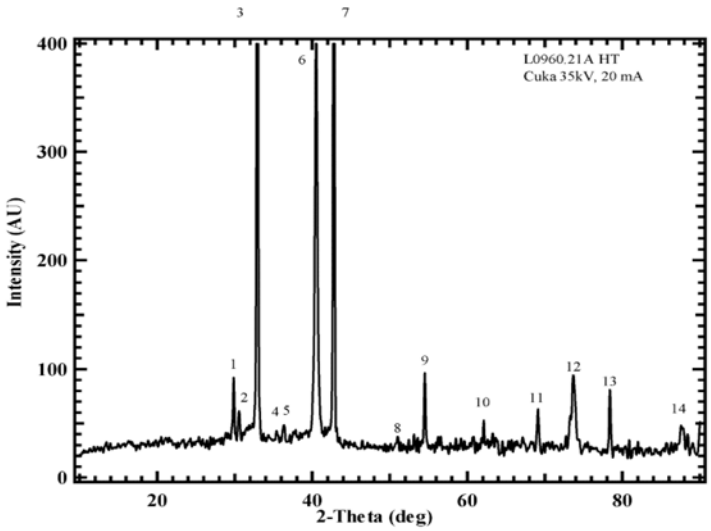

Figure 3. XRD spectrum of Cu-Ga-In precursor heat-treated for 10 min at 450ºC.

Table II. Peak indexing of heat-treated Cu-Ga-In precursor shown in Figure 1.

Peak	2θ (º)	d(Å)	Index
1	29.85	2.991	$Cu_9(Ga_{0.36}In_{0.64})_4$ (300)
2	30.55	2.924	In_2O_3 (222)
3	32.90	2.720	In (100)
4	35.40	2.533	In_2O_3 (400)
5	36.35	2.469	In (002)
6	40.50	2.225	Mo (110)
7	42.75	2.113	$Cu_9(Ga_{0.36}In_{0.64})_4$ (411)
8	51.00	1.789	In_2O_3 (440)
9	54.50	1.682	In (112)
10	62.10	1.493	$Cu_9(Ga_{0.36}In_{0.64})_4$ (600)
11	69.10	1.358	In (202)
12	73.65	1.285	Mo (221)
13	78.35	1.219	$Cu_9(Ga_{0.36}In_{0.64})_4$ (552)
14	87.55	1.113	Mo (220)

Analysis of $Cu(InGa)Se_2$ films

$Cu(InGa)Se_2$ films were formed by reactions in a quartz tube reactor at 450°C in 1 atm flowing Ar with 0.35% hydride gas and 0.0035% O_2 for reaction times of 10, 30, and 90 min. The quartz tube was ramped to the reaction temperature from 0 to 10 min, and then allowed to thermally stabilize from 10 to 20 min. Ar/0.0035% O_2 was flowed during the temperature ramp and stabilization. The samples were held outside of the reaction zone during this time, so that their temperature was <50°C. For reactions, the H_2Se flow was begun at 17 min. Samples were pushed into the reaction zone at 20 min, and pulled out after the desired reaction time. Previous

measurements indicated that the samples require approximately 5 min to fully reach temperature upon insertion into the reaction-zone.

A unique aspect of this work is the liftoff of the selenized films to allow analysis of the $Cu(InGa)Se_2$ backside and the exposed Mo back contact. The surface morphology of the selenized films, shown in Figure 4, did not show a significant change with increasing reaction time. The backside morphologies of the peeled films, shown in Figure 5, exhibited significant voiding at all reaction times. EDS measurements, listed in Table III, indicated little Ga content, with $Ga/(In+Ga) \leq 0.03$, when measured from the front side and no change with increasing reaction time. EDS measured from the backsides of the films indicated steady increase in both Cu and Ga (Table III).

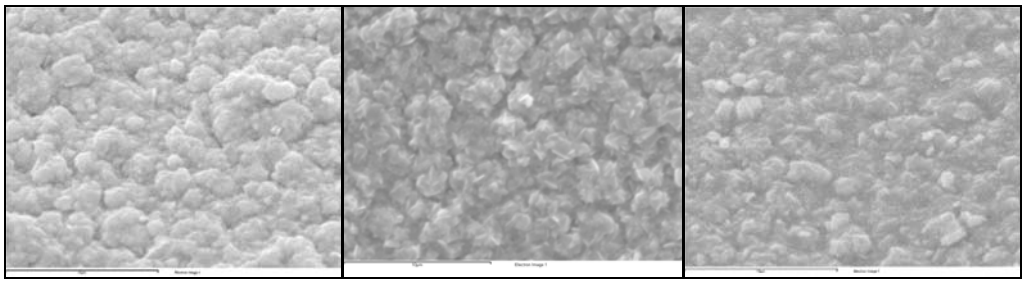

Figure 4. SEM micrographs of films selenized for 10 (left), 30 (center), and 90 min (right). Images are ~ 20 µm across.

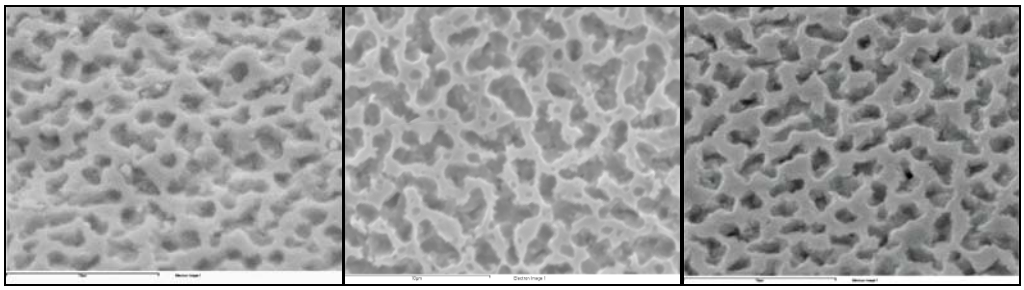

Figure 5. Backsides of peeled films selenized for 10 (left), 30 (center), and 90 min (right). Images are ~ 20 µm across.

Table III. Composition of front- and backsides of selenized films.

H_2Se time (min)	Front side			Backside		
	$\frac{Cu}{In + Ga}$	$\frac{Ga}{In + Ga}$	Se (at. %)	$\frac{Cu}{In + Ga}$	$\frac{Ga}{In + Ga}$	Se (at. %)
10	0.96	0.03	46.5	0.53	0.16	44.2
30	1.00	0.02	46.2	0.71	0.42	47.9
90	1.01	0.02	46.4	0.81	0.48	47.3

Inspection of the Mo back contact after $Cu(InGa)Se_2$ peel-off revealed residual nodules as shown in Figure 6. EDS measurements shown in Table IV indicate that the nodules contained little Se. The measurements at all three reaction times indicate a Cu/(Ga+In) ratio of approximately 1.85. The intermetallic at 10 min has a small amount of In, while those at 30 and 90 min are comprised solely of Cu and Ga.

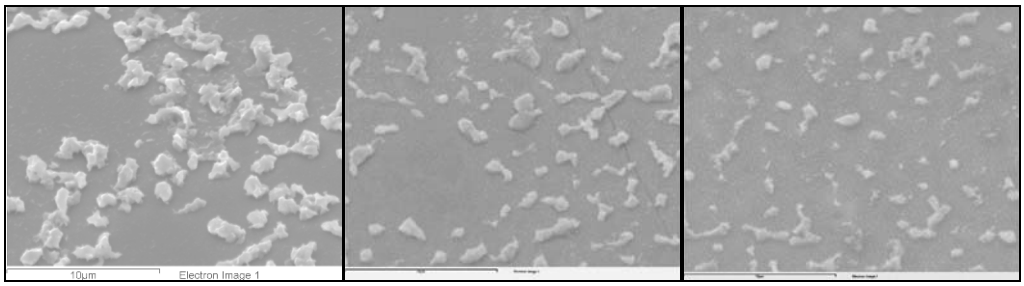

Figure 6. Residual intermetallics on Mo back contact after peeling of $Cu(InGa)Se_2$ films. L to R: 10, 30, 90 min reaction time. Images are ~ 20 µm across.

Table IV. Composition of residual intermetallics on Mo back contact.

Se time (min)	Cu at%	In at%	Ga at%	Se at%	$\frac{Cu}{In + Ga}$	$\frac{Ga}{In + Ga}$
10	52.8	6.5	21.4	3.2	1.89	0.77
30	52.1	0.0	27.5	0.8	1.90	1.00
90	42.9	0.05	24.4	1.2	1.76	1.00

These results indicate the incongruent reaction of Cu-Ga-In intermetallics in H_2Se, with the extraction of In being favored over that of Ga. Qualitatively, the slow depletion of the Cu-Ga intermetallic phase correlates with the slow incorporation of Cu and Ga into the backside of the $Cu(InGa)Se_2$ film. The segregation caused by the preferred reaction of In may be a contributing mechanism to the migration of Ga to the backside of selenized Cu-Ga-In precursor films.

Fundamental Materials and Interface Characterization

Optical Characterization

A paper "Analysis of Cu(InGa)Se_2 Alloy Film Optical Properties and the Effect of Cu Off-Stoichiometry" by P.D. Paulson, S.H. Stephens, and W.N. Shafarman was presented at the 2005 MRS Spring meeting. In this work, variable angle spectroscopic ellipsometry (SE) was used to characterize Cu(InGa)Se_2 thin films as a function of Cu off-stoichiometry in films with $0.3 \leq$ Cu/(In+Ga) ≤ 1 and Ga/(In+Ga) = 0.3. Films with Cu/(In+Ga) less than ~ 0.9 but greater than ~ 0.5 are expected to contain 2 phases, by analogy with the $CuInSe_2$ phase diagram.[1] SE measurements were made over the energy range of 0.75–4.6 eV using the procedure described previously.[2] Mo was deposited on the exposed surface of the CIGS and then the films were peeled to expose the CIGS back surface, providing a smooth surface for characterization.

First, the optical constants n and k of films assumed to contain single phase α-CIGS (Cu(InGa)Se_2) with 24.8 at.% Cu and single phase δ_R-CIGS with 10.4 at.% Cu were determined, using an oscillator model similar to that used in Reference 2. These are shown in Figure 7. Mixed phase films with intermediate Cu concentrations were then modeled using an effective medium approximation (EMA) in which the optical constants were determined as a mixture of the constants for the α-CIGS and δ_R-CIGS. This gave comparable results to an oscillator model, which treats the films as single phase, as shown by the comparison for 2 films in Figure 8. In particular, there is good agreement for all critical point energies that correspond to the optical transitions in the material. The volume fractions of the α and δ_R phases used for the EMA fits are indicated in the figures. The volume fractions are consistent, within experimental uncertainty, with the compositions measured by EDS.

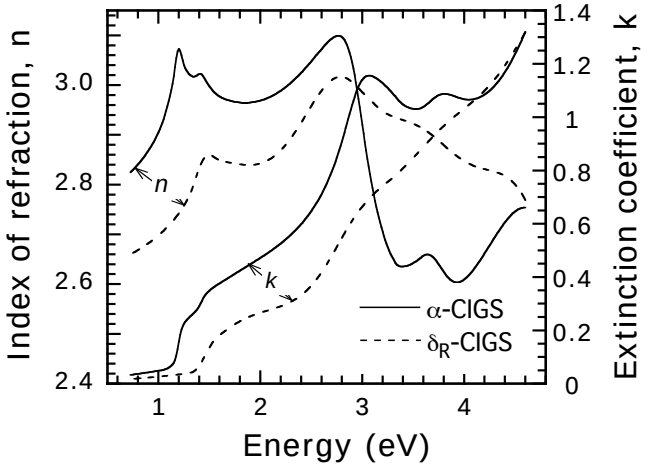

Figure 7. Optical constants of α-CIGS and δ_R-CIGS films with Ga/(In+Ga) = 0.3.

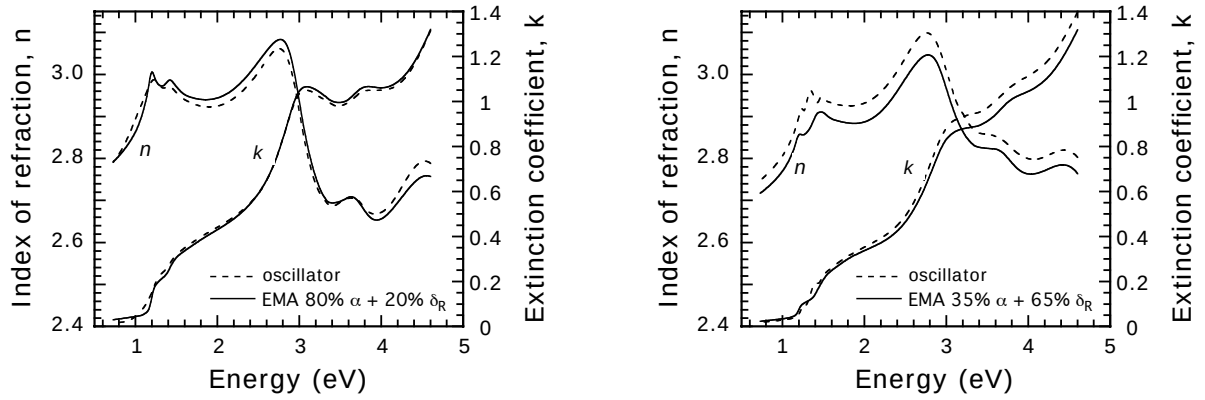

Figure 8. Comparison of optical constants obtained using an oscillator model and EMA model for films in the $\alpha + \delta_R$ mixed phase region. The film on the left has 22.0% Cu and the film on the right has 18.6% Cu.

The optical constants determined by the EMA model are shown in Figure 9 for a set of 6 mixed phase films with different Cu compositions. Two distinctive features are observed in the optical spectra as the Cu concentration decreases. First, the fundamental bandgaps are shifted to higher energies. Second, the critical point features at higher energies become broader suggesting degradation of the crystalline quality of the material.

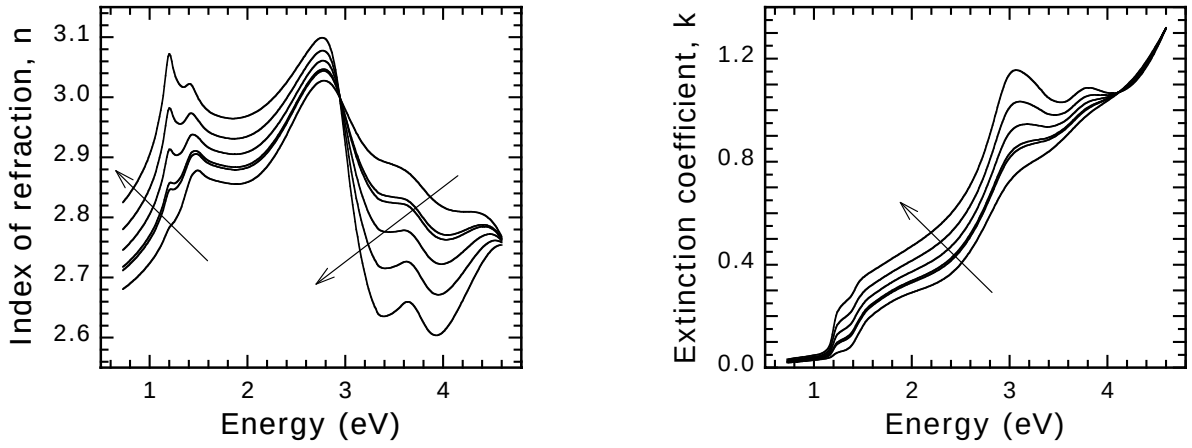

Figure 9. Optical constants of CIGS films with Ga/(In+Ga) = 0.3 determined by EMA analysis. Arrows indicate increasing Cu (%) in sequence 23.6, 22.0, 20.7, 18.6, 15.4, 11.6.

References

[1] T. Gödecke, T. Haalboom and F. Ernst, Z. Metallkd. **91**, 622 (2000).
[2] P.D. Paulson, R.W. Birkmire, W.N. Shafarman, J. Appl. Phys. **94**, 879 (2003).

Best regards,

Robert W. Birkmire
Director

RWB/bj
Cc: Gerri Hobbs, UD Research Office
Carolyn Lopez, NREL
Paula Newton
Erten Eser
William N. Shafarman